

Treating uncertainties in a nuclear seismic probabilistic risk assessment by means of the Dempster-Shafer theory of evidence

*Original*

Treating uncertainties in a nuclear seismic probabilistic risk assessment by means of the Dempster-Shafer theory of evidence / Lo Chung, Kung; Pedroni, Nicola; Zio, E.. - In: NUCLEAR ENGINEERING AND TECHNOLOGY. - ISSN 1738-5733. - 46:1(2014), pp. 11-26. [10.5516/NET.03.2014.701]

*Availability:*

This version is available at: 11583/2672027 since: 2017-05-24T18:08:33Z

*Publisher:*

Korean Nuclear Society

*Published*

DOI:10.5516/NET.03.2014.701

*Terms of use:*

This article is made available under terms and conditions as specified in the corresponding bibliographic description in the repository

*Publisher copyright*

(Article begins on next page)

# TREATING UNCERTAINTIES IN A NUCLEAR SEISMIC PROBABILISTIC RISK ASSESSMENT BY MEANS OF THE DEMPSTER-SHAFER THEORY OF EVIDENCE

CHUNG-KUNG LO<sup>1</sup>, N. PEDRONI<sup>2</sup>, and E. ZIO<sup>1,2\*</sup>

<sup>1</sup>Chair on Systems Science and the Energetic Challenge,

European Foundation for New Energy - Electricité de France, at École Centrale Paris - Supélec, France

<sup>2</sup>Department of Energy, Politecnico di Milano, Italy

Corresponding author. E-mail : enrico.zio@ecp.fr

*Received January 10, 2014*

---

The analyses carried out within the Seismic Probabilistic Risk Assessments (SPRAs) of Nuclear Power Plants (NPPs) are affected by significant aleatory and epistemic uncertainties. These uncertainties have to be represented and quantified coherently with the data, information and knowledge available, to provide reasonable assurance that related decisions can be taken robustly and with confidence. The amount of data, information and knowledge available for seismic risk assessment is typically limited, so that the analysis must strongly rely on expert judgments. In this paper, a Dempster-Shafer Theory (DST) framework for handling uncertainties in NPP SPRAs is proposed and applied to an example case study. The main contributions of this paper are two: (i) applying the complete DST framework to SPRA models, showing how to build the Dempster-Shafer structures of the uncertainty parameters based on industry generic data, and (ii) embedding Bayesian updating based on plant specific data into the framework. The results of the application to a case study show that the approach is feasible and effective in (i) describing and jointly propagating aleatory and epistemic uncertainties in SPRA models and (ii) providing ‘conservative’ bounds on the safety quantities of interest (i.e. Core Damage Frequency, CDF) that reflect the (limited) state of knowledge of the experts about the system of interest.

---

KEYWORDS : Seismic Probabilistic Risk Assessment, Dempster-Shafer Theory, Bayesian Update, Uncertainty, Probability Box, Belief and Plausibility Functions

## 1. INTRODUCTION

A Nuclear Power Plant (NPP) Seismic Probabilistic Risk Assessment (SPRA) [1] aims at estimating the probability of occurrence of different sizes of earthquakes that may affect the NPP and assesses the NPP response to such earthquakes. The results of the assessment are presented in terms of seismically induced Core Damage Frequency (CDF) and Large Early Release Frequency (LERF). SPRA is a multi-disciplinary activity combining the inputs and experience of different specialized domain disciplines, such as seismic hazard analysis, seismic fragility evaluation and system analysis, under the normative umbrella of risk analysis.

All the analyses carried out in SPRA are affected by uncertainties: in general, these can be categorized as either aleatory or epistemic. Aleatory uncertainty reflects our inability to predict random observable events, whereas epistemic uncertainty represents the analyst lack of knowledge of the values of (constant) parameters (e.g. probabilities, failure rates, ...) that are used in the model for a particular SPRA task. These uncertainties have to be represented

coherently with the data, information and knowledge available, and propagated onto the risk measures of interest (i.e. CDF and LERF) in order to establish the level of confidence that can be placed in the decisions or conclusions taken, based on the results of the assessment. Then, the aim of analyzing the uncertainties and assessing their impact onto the SPRA results is to provide reasonable assurance that the decisions taken based on such results are robust, and would therefore not warrant reconsideration.

In the traditional SPRA practice both types of uncertainty, aleatory and epistemic, are represented by probability distributions. However, the choice of a probability distribution (e.g. lognormal, gamma or beta) for representing epistemic parameter uncertainty due to imprecise and incomplete data is somewhat arbitrary and often made because of conventional reasons and simplifying assumptions [2]. On the other hand, various recent studies [3, 4] have recognized that it may be more appropriate to use a set (i.e. a family) of probability distributions to represent incomplete and imprecise information about a parameter, rather than a unique presumed probabilistic distribution. Such a family can be represented by probability boxes

(p-boxes), possibility distributions or belief/plausibility functions within the paradigm of Dempster-Shafer Theory (DST). The DST appears as an appealing framework for uncertainty treatment because it allows a very flexible uncertainty representation and it has a well-established connection to many other frameworks. In the early stages of DST, the application was mainly focused on data fusion and artificial intelligence [5, 6]. The studies of its application to complex industrial systems are still limited. Recently, a framework using the DST for dealing with uncertainties in the context of NPP risk analysis has been proposed and developed [7]. Within this framework, the intention of this paper is to demonstrate how to treat uncertainty using the DST in NPP SPRA.

The paper is organized as follows. In section 2, we introduce the logic scheme of the NPP SPRA and the necessary basic information of each phase such as seismic hazard analysis, component fragility evaluation etc.. In section 3, we outline briefly the methodology for uncertainty treatment, demonstrate the building of the Dempster-Shafer structure for some simple general cases and introduce the process of Bayesian updating, when data becomes available. Section 4 presents the steps to build the Dempster-Shafer structure to represent the uncertainty of the parameters appearing in the different SPRA analyses and the framework for propagation. In Section 5, the proposed approach is practically illustrated on a simplified NPP SPRA model. Finally, some conclusions and perspectives are discussed in Section 6.

## 2. BASICS OF NPP SPRA

SPRA is a multi-disciplinary activity combining the inputs and experience of different specialized domain disciplines, such as seismic hazard analysis, seismic fragility evaluation and system analysis, onto a risk analysis framework [1]. Steps to perform NPP SPRA include:

- Probabilistic analysis of the Seismic Hazards of the plant site.
- Evaluation of the seismic fragility of the system components.
- Construction of SPRA logic model of the NPP.
- Propagation of aleatory and epistemic uncertainties.

For completeness of the paper, each of these steps is described briefly in the subsections below.

### 2.1 Probabilistic Seismic Hazard Analysis

A basic prerequisite for performing a SPRA for a facility located at a given site is the development of seismic hazard curves associated with that site. A seismic hazard curve presents the annual frequency of exceedance of a given threshold for different values of a selected ground motion parameter. Hazard curves, which are used as input data in the SPRA, are the final output of a Probabilistic Seismic Hazard Analysis (PSHA) [8], which results in the com-

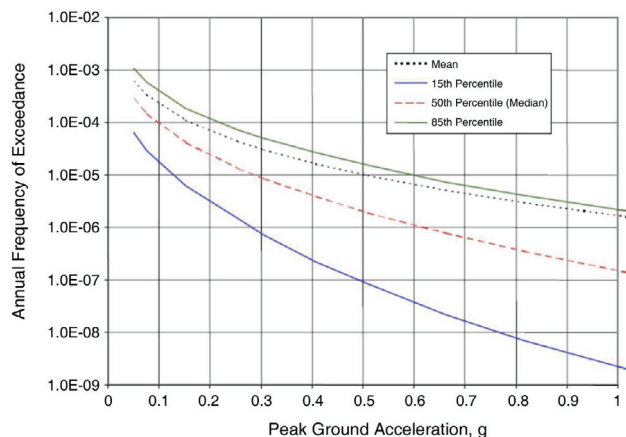


Fig. 2-1. Example of Hazard Curves for PGA

putation of the mean annual frequency of exceedance for the selected ground motion parameter and the associated uncertainty at a particular site. The uncertainty is due to both randomness (aleatory uncertainty) and lack of knowledge about the earthquake phenomenon affecting the site (epistemic uncertainty).

The hazard curves developed by a PSHA represent the aggregate hazard from potential earthquakes of many different magnitudes occurring at many different source-site distances. The conduction of a PSHA represents a substantial effort in both time and cost, and it involves the contributions of several specialists in the areas of geology, seismology, and geotechnical engineering. PSHA involves the following basic steps:

- Identification and characterization of earthquake source zones, which are capable of producing significant ground motions at a specific site.
- Construction of a model describing the temporal distribution or recurrence of earthquakes within each source zone, commonly expressed in terms of frequency of occurrence versus a measure of earthquake size.
- Construction of a model describing the conditional distribution of the strong motion parameter of interest for a specific site, given the occurrence of an earthquake of given magnitude and distance. The predictive relationships of motion parameter for various source events in terms of magnitude and site distance, are referred to as ground motion attenuation relationships.
- Integration of the first three steps to produce the hazard curves for the chosen site.

Hazard curves are usually presented in terms of the annual frequency of occurrence for a given site versus a ground motion parameter, such as Peak Ground Acceleration (PGA). The presentation of the resulting curve has on the ordinate axis the logarithm of the occurrence frequency and on the abscissa axis the linear value of the ground motion parameter. The variability in the hazard is shown by plotting the percentiles of the hazard curve, as shown in Figure 2-1. For example, the 85% percentile curve

**Table 2-1.** Tabular Presentation Format of PSHA Results

| Annual probability of exceedance | PGA    |        |        |
|----------------------------------|--------|--------|--------|
|                                  | 10%    | 50%    | 90%    |
| 8.11E-01                         | 0.0082 | 0.0106 | 0.0129 |
| 5.57E-01                         | 0.0149 | 0.0187 | 0.0224 |
| ...                              | ...    | ...    | ...    |
| ...                              | ...    | ...    | ...    |
| 5.17E-07                         | 0.7249 | 1.1804 | 1.6358 |
| 2.52E-07                         | 0.7500 | 1.2086 | 1.6673 |

defines the motion level that has a 15% chance of being exceeded or alternatively the level that will not be exceeded with a confidence of 85%. A tabular presentation (see Table 2-1) of the hazard analysis results, supplemented by a few hazard curves, is a preferred presentation format for PSHA results.

Traditionally, most NPP SPRA models only use a single hazard curve (50% or mean). This implies treating the ground motion parameter as a random (aleatory) variable, only. The (single) hazard curve is, then, used to combine all calculated results of conditional core damage probability (CCDP) for different PGA values, to generate the CDF distribution induced by the seismic hazard.

### 2.2 Seismic Fragility Evaluation and Estimation of Components Failure Probabilities

The objective of a fragility evaluation [9] is to estimate the capacity of resistance of components with respect to a given value of the ground motion parameter. The capacity is represented by fragility curves. A fragility curve depicts the conditional probability of failure of the component for any given ground motion level. In Figure 2-2, it can be seen that the conditional failure probability of a component increases with the ground motion level to which the site may be subjected to, approaching 1.0 at high accelerations.

The output of the fragility analysis is a set of three fragility parameters, the median capacity  $A_m$ , the logarithmic standard deviation of randomness  $\beta_R$  and the logarithmic standard deviation of uncertainty  $\beta_U$ , for each component important to seismic analysis. With perfect knowledge of the failure mode and parameters describing the ground acceleration capacity (i.e. only accounting for the random variability,  $\beta_R$ , and setting the state of knowledge uncertainty parameter,  $\beta_U$ , equal to zero), the conditional probability of failure,  $f_0$ , for a given PGA value,  $a$ , is given by:

$$f_0 = \Phi \left[ \frac{\ln\left(\frac{a}{A_m}\right)}{\beta_R} \right] \quad (2-1)$$

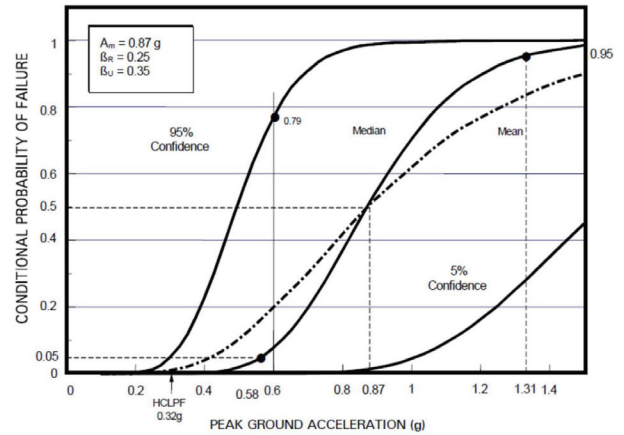


**Fig. 2-2.** Example of Fragility Curves for a Component

where  $\Phi[\cdot]$  is the standard Gaussian cumulative distribution function of the term in brackets.

The relationship between  $f_0$  and  $a$  is the median fragility curve, plotted in Figure 2-2 for a component with a median ground acceleration capacity  $A_m = 0.87g$  and  $\beta_R = 0.25$ . For a median conditional probability of failure value ranging from 5% to 95%, (- and + 1.65 logarithmic standard deviations of randomness), the ground acceleration capacity ranges from  $A_m \exp(-1.65\beta_R)$  to  $A_m \exp(1.65\beta_R)$ , i.e. from 0.58g to 1.31g as shown in Figure 2-2.

When the state-of-knowledge uncertainty  $\beta_U$  is included, the fragility at a specific acceleration value becomes an uncertain variable. At each acceleration value  $a$ , the fragility is now represented by the subjective probability  $Q$  (also known as “confidence” ranging from 0 to 1) of not exceeding a fragility  $f'$ . The terms  $Q$  and  $f'$  are related by the following equation:

$$f' = \Phi \left[ \frac{\ln\left(\frac{a}{A_m}\right) + \beta_U \Phi^{-1}(Q)}{\beta_R} \right] \quad (2-2)$$

where  $Q = P(f < f' | a)$  is the subjective probability (confidence) that the conditional probability of failure,  $f$ , is lower than  $f'$  for a PGA value  $a$ , and  $\Phi^{-1}[\cdot]$  is the inverse of the standard Gaussian cumulative distribution of the term in brackets.

For example, the conditional probability of failure  $f'$  at a PGA of 0.6g that has a 95% subjective probability (confidence) of not being exceeded is obtained from Equation (2-2) as 0.79, as shown in Figure 2-2 on the 95% confidence curve. The 5% to 95% probability (confidence) interval on the failure probability at 0.6g is [0, 0.79]. A mean fragility curve is also plotted in Figure 2-2. This is obtained using Equation (2-1), by replacing  $\beta_R$  with the composite variability  $\beta_C = (\beta_R^2 + \beta_U^2)^{1/2}$ .

The fragility data of components are used to evaluate the probabilities of the seismic damage states (SDSs), given an occurred earthquake.

### 2.3 Construction of the SPRA Logic Model of the NPP

The objective of SPRA is to assess the NPP response to earthquakes. To achieve this goal, we have to construct a logic model to evaluate the seismic induced CDF and LERF. In NPP practice, a seismic equipment list (SEL) is used to define the analysis scope of SPRA, including the equipment and systems required to provide protection for all seismically induced initiating events and the structures that house them. The structures and equipment listed in SEL are considered for fragility evaluation. A seismic event tree (SET) is constructed to define the SDSs according to the combination of headings (top events) successes and failures, given an occurred earthquake.

An example of SET is shown in Figure 2-3. The headings (top events) in the SET are failures of structures and equipment in the SEL. The SDSs in the SET include success (OK), core damage (CD), and the occurrence of seismic initiating events (e.g. loss of outside power, loss of coolant etc.). The OK means the plant safety is not challenged by the seismic hazard and the CD means the plant suffers core damage given an earthquake has occurred. To evaluate the CDF and LERF under the seismic conditions, the frequencies of occurrence of the seismic initiating events must be combined with the non-seismic failure probabilities of the mitigation and safety systems still available after the earthquake.

Only the seismic induced impacts on the plant are considered in the SET. The success of a heading event in the SET (hence, the success of the equipment which the heading refers to) means that the equipment does not fail due to seismic ground motion. However, it may still fail from non-seismic failure causes. For seismic initiating events, the non-seismic failures (e.g., random hardware failure or operator errors) are evaluated in a separate event tree from the internal events accident sequence model.

The CCDPs for each seismic initiating event are based on an internal Probabilistic Risk Assessment (PRA) model, typically made by event trees and system fault trees. Since the CCDPs are seismic independent, they can be developed in advance and treated as plant level parameters.

For the evaluation of non-seismic failures in the internal events model, we have to estimate the random failure probabilities of the components. In general, the component generic data in the nuclear industry is often provided in terms of the most likely value of the variable (mean)

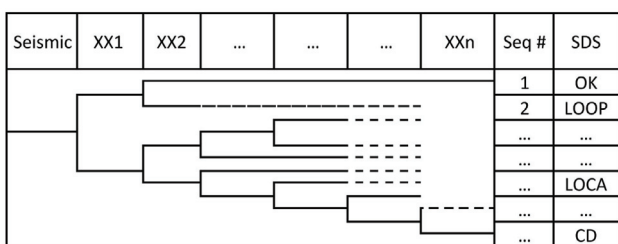


Fig. 2-3. Example of SET

with a confidence interval (5% and 95% percentiles). The possible values of the parameters are obtained from statistical estimation methods, such as the Maximum likelihood Estimation or the Bayesian estimation [2]. The uncertainty associated to the parameters is generally represented by presumed probability distributions (such as the log-normal, gamma or beta distributions), which express a subjective confidence of the analyst in the possible parameter values. Such uncertainty treatment scheme allows Bayesian updating when plant specific data is available.

### 2.4 Propagation of Uncertainty through the Logic Model

The total seismic induced CDF accounts for the core damage due directly to the seismic hazard and the core damage resulting from the accident sequence that developed from the seismic initiating events. The overall seismic risk quantification process presented in Figure 2-4 shows the propagation of uncertainty through the logic model under assessment.

The first step of performing the risk quantification is top event evaluation. In this step, the fault tree associated with each top event (heading) included in the SET is used to determine the conditional probability of the top event. This is done over a specific interval of ground motion values that the plant site may be subjected to. The individual component conditional failure probabilities for each top event are combined to determine the conditional probability of the top event: this is referred to as top event level fragility curve for each top event.

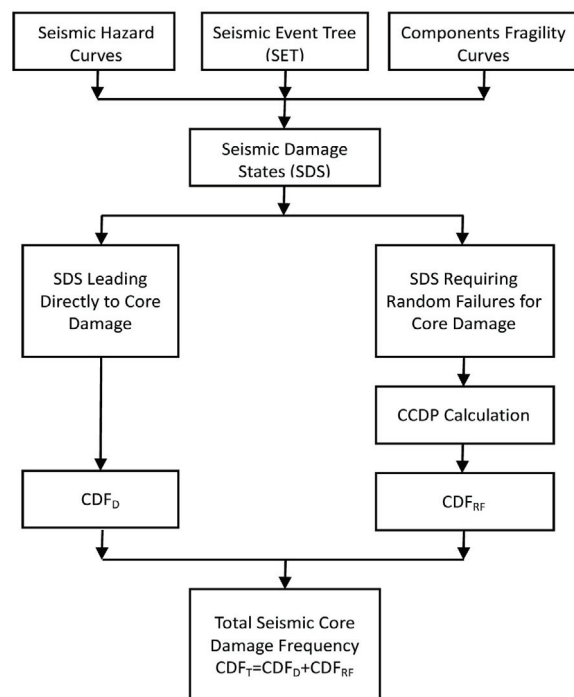


Fig. 2-4. SPRA Process

The second step is the SET sequence quantification. In this step, we compute the sequence level fragility curves for each sequence defined in the SET according to the combination of top events along the sequence. As top events, the sequence level fragility curves are calculated over a specific interval of ground motion that the plant site may be subjected to.

The third step is the quantification of the core damage probability induced by seismic initiating event sequences. In this step, the sequence level fragility curves for each seismic initiating event are combined with the associated non-seismic event tree CCDP distribution to generate the core damage fragility curves. These core damage fragility curves of seismic initiating events are, then, combined with the sequence level fragility curves of core damage directly induced by the seismic hazard, to get the plant level core damage fragility curves.

The final step is the estimation of the CDF: the plant level fragility curves are combined with the seismic hazard curves to fulfill the seismic risk assessment.

### 3. BASICS OF DST AND POSSIBILISTIC BAYESIAN UPDATING PROCESS

It is claimed that the data, information and knowledge typically available for the analysis involved in NPP SPRA is typically limited and challenge a (single distribution) probabilistic treatment of epistemic uncertainty. Then, the main purpose of this paper is to show the treatment of uncertainty by DST in NPP SPRA based on data information and knowledge available. Since plant specific data brings information for uncertainty analysis, we consider also Bayesian updating. In this section, we outline briefly the DST and Bayesian updating.

#### 3.1 Dempster-Shafer Theory

The DST of evidence [10], also known as the theory of belief functions, is a generalization of the Bayesian theory of subjective probability in that it allows less restrictive assumptions about the likelihood, than in the case of a probabilistic characterization of uncertainty.

The DST is a mixed representation, which combines the probabilistic representation and the interval representation in a single representation. Over the set of the real numbers, the DST resembles a discrete probability theory except that the locations at which the probability mass resides are sets of real values, rather than precise points. These sets associated with non-null mass are called focal elements. Typically, focal elements are chosen among closed intervals also called focal intervals. The correspondence of probability masses associated with the focal intervals is called the basis belief assignment (BBA), noted  $m$ . In the DST, this BBA on the real line is a mapping such that  $m: 2^{\mathbb{R}} \rightarrow [0,1]$  where  $m(\emptyset) = 0$  and  $\sum_{A \subseteq \mathbb{R}} m(A) = 1$ , for all subsets  $A$  of  $\mathbb{R}$ . The BBA for a given set can be understood as the weight of evidence that the truth is in that set, evidence which cannot be further subdivided on the basis of the data information and knowledge available. Unlike a discrete probability distribution where the mass is concentrated at distinct points, the focal intervals in DST may overlap one another (see on Figure 3-1). As can be seen in this Figure, the uncertainty associated with an epistemic variable  $X$  can be represented by the so-called Dempster-Shafer structure as:

$$\{([a_1, b_1], m_1), ([a_2, b_2], m_2), \dots, ([a_n, b_n], m_n)\} \quad (3-1)$$

where  $a_i \leq b_i$ ,  $\sum_{i=1}^n m_i([a_i, b_i]) = 1$  and  $[a_i, b_i] \subseteq \mathbb{R} \forall i \leq n$ . The Dempster-Shafer structure is, thus, a collection of pairs consisting of closed intervals and corresponding BBAs. From a computational point of view, this construction is helpful for propagating the uncertainty through a given model function by simulation.

Associated with each BBA are two functions,  $Bel$  and  $Pl$ , which are referred to as belief and plausibility functions. The belief and plausibility functions of uncertain variable  $X$  belonging to a subset  $[b, \bar{b}] \subseteq \mathbb{R}$  are defined as:

$$Bel(X \in [b, \bar{b}]) = \sum_{[a_i, b_i] \subseteq [b, \bar{b}]} m([a_i, b_i]) \quad (3-2)$$

$$Pl(X \in [b, \bar{b}]) = \sum_{[a_i, b_i] \cap [b, \bar{b}] \neq \emptyset} m([a_i, b_i]) \quad (3-3)$$

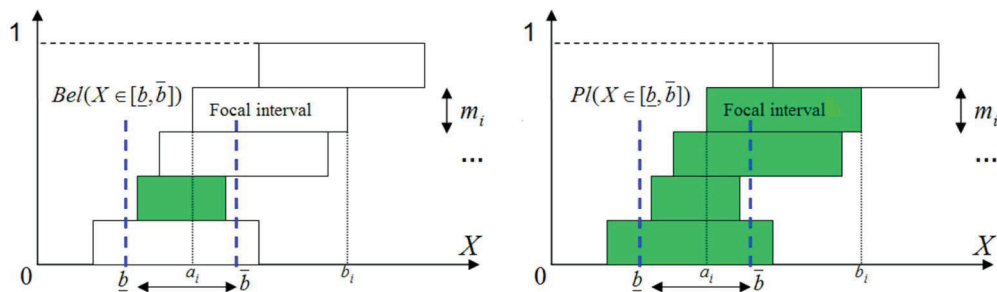


Fig. 3-1. An Example of Belief and Plausibility Functions

The belief function  $Bel(X \in [\underline{b}, \bar{b}])$  represents the degree of belief, based on the available evidence (e.g., given focal intervals  $[a_i, b_i]$ ), that the true value of variable  $X$  belongs to  $[\underline{b}, \bar{b}]$ . On the other hand, the plausibility function  $Pl(X \in [\underline{b}, \bar{b}])$  can be interpreted as the total evidence that the true value of variable  $X$  belongs not only to  $[\underline{b}, \bar{b}]$ , as for  $Bel(X \in [\underline{b}, \bar{b}])$ , but also to any other given focal interval which overlaps with  $[\underline{b}, \bar{b}]$ . When the focal intervals are reduced to precise values, the belief and plausibility functions coincide with the cumulative distribution function (cdf) of probability theory.

The belief and plausibility functions are recognized to be the lower and upper bounds of the cdf. In fact, according to the imprecise probabilities theory [11], the imprecision in the cumulative distribution function is characterized by lower and upper cdfs  $[\underline{F}, \bar{F}]$  (named a p-box), such that  $\underline{F}(x) \leq F(x) \leq \bar{F}(x)$  where  $F(x) = P(X \leq x)$  is the cdf (probabilistic). Given a Dempster-Shafer structure as in Equation (3-1), these two functions are equated with the cumulative belief and plausibility functions and defined as:

$$\underline{F}(x) = Bel(X \in (-\infty, x]) = \sum_{b_i \leq x, i=1}^n m([a_i, b_i]) \quad (3-4)$$

$$\bar{F}(x) = Pl(X \in (-\infty, x]) = \sum_{a_i \leq x, i=1}^n m([a_i, b_i]) \quad (3-5)$$

Thus, we can see that the (probabilistic) cdf  $F(x) = P(X \leq x)$  is bounded by the cumulative belief and plausibility functions see Figure 3-2. Inversely, since a unique p-box,

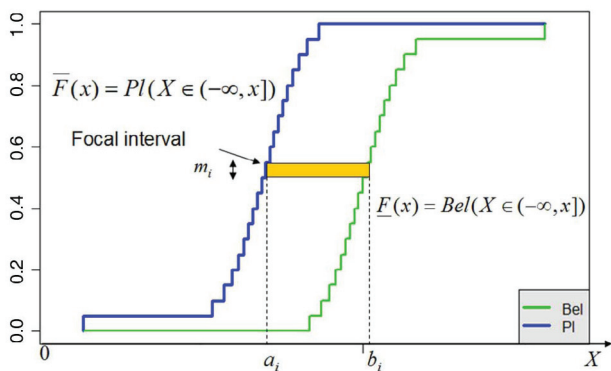


Fig. 3-2. Cumulative Belief and Plausibility Functions

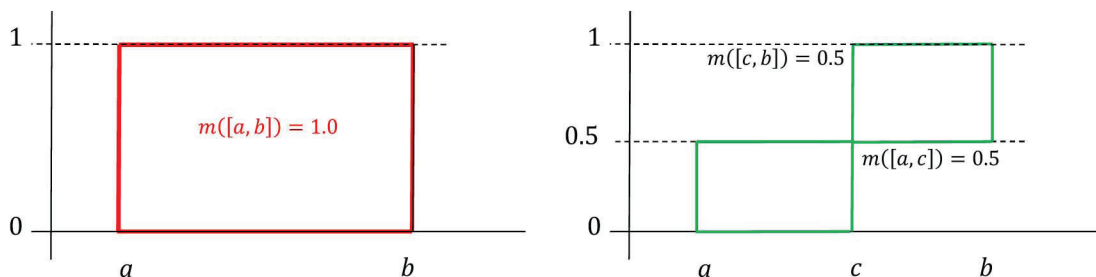


Fig. 3-3. Dempster-Shafer Structure Based on Range and Median Value

$[\underline{F}, \bar{F}]$ , can induce many Dempster-Shafer structures, in practice a Dempster-Shafer structure is often approximately obtained using discretization techniques [12].

The DST is also related to the possibility theory which can be seen as an extension of the fuzzy set theory. In the possibility theory, uncertainty is represented by a possibility distribution which is equivalent to the belief functions of DST when the focal intervals are nested. Therefore, it is recognized that the possibility theory is a special case of the DST [13]. The relationship between the possibility theory and the DST is very important for the Bayesian updating process, as we shall see in section 3.3 below.

### 3.2 Building Dempster-Shafer Structure Based on Available Information

In the absence of specific data, precise information and sure knowledge, it seems more reasonable to specify a possible range of values for a variable rather than a single, point value. To clarify this, in the following, we consider a handful of examples of commonly encountered situations. Suppose, for example, that it is known that an uncertain parameter cannot be smaller than nor larger than : then, the interval  $[a, b]$  is used and the associated Dempster-Shafer structure is  $\{([a, b], 1)\}$  (Figure 3.3). If the median  $c$  of an uncertain variable is also known, this pinches the uncertainty distribution to a definite point at the 50% probability level. As shown in Figure 3-3, the associated Dempster-Shafer structure for this case is  $\{([a, c], 0.5)\}$ ,  $\{([c, b], 0.5)\}$ . Having reliable knowledge of other percentiles would correspond to similar structures. The focal intervals in this case do not overlap.

If in addition to the range, the mean of a random variable is also known, the p-box can be further refined. Let  $x_{inf}$ ,  $x_m$  and  $x_{sup}$  be the minimum, mean and maximum values respectively. First, consider the  $x$ -values between the minimum and the mean. The upper bound on probability over this range can be found by determining the largest possible values attained by a distribution function under the specified constraints [12]. Consider an arbitrary value  $x \in [x_{inf}, x_m]$ , the value  $p$  of a distribution function at  $x$  represents the probability mass at and to the left of  $x$ . The probability mass on the left must be balanced by the mass on the right of the mean. The greatest possible mass would

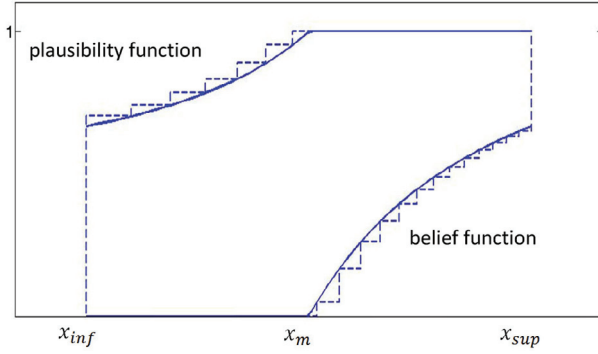


Fig. 3-4. Dempster-Shafer Structure Based on Range and Mean

be balanced by assuming that the rest of the probability,  $1 - p$ , is concentrated at  $x_{sup}$ . Likewise, the arrangement of mass on the left side requires the least balance when it is all concentrated at the point  $x$ . These considerations lead to the expression which can be solved to yield  $px + (1 - p)x_{sup} = x_m$ , which can be solved to yield  $p = (x_{sup} - x_m)/(x_{sup} - x)$ , specifying the largest value of the distribution function for the value  $x$ . If there were any more probability mass at values less than or equal to  $x$ , the constraint of the mean could not be satisfied by any arrangement of mass at values less than or equal to  $x_{sup}$ . Clearly, then, the spike distributions defined by this expression describe the bounding distribution over the range  $[x_{inf}, x_m]$ , subject to the fundamental constraint  $0 \leq p \leq 1$ . The position of the lower bound is determined by the degenerate distribution which has all its mass at the mean. Its distribution function is zero from  $x_{inf}$  to  $x_m$ . Lower and upper bounds for values larger than  $x_m$  can be derived by similar (but inverted) arguments. The resulting p-box is, then,  $[F, \bar{F}]$ , where

$$\underline{F}(x) = \begin{cases} \frac{x - x_m}{x - x_{inf}} & \forall x \in [x_m, x_{sup}] \\ 0 & \forall x \in [x_{inf}, x_m] \end{cases} \quad (3-6)$$

$$\bar{F}(x) = \begin{cases} 1 & \forall x \in [x_m, x_{sup}] \\ \frac{x_{sup} - x_m}{x_{sup} - x} & \forall x \in [x_{inf}, x_m] \end{cases} \quad (3-7)$$

The belief and plausibility functions of this case are plotted in Figure 3-4. As shown in Figure 3-4, the associated Dempster-Shafer structure can be obtained by canonical discretization [12].

### 3.3 Possibilistic Bayesian Updating Process

The possibilistic Bayesian updating process has already been proposed in the literature [14]. As mentioned in the previous section, in possibility theory, uncertainty is represented by a possibility distribution which is equivalent to the belief functions of the DST when the focal intervals are nested. We can transform the belief and plausibility functions of parameter  $X$ , obtained based on industry generic

data, to an equivalent possibility distribution and embed the possibilistic Bayesian updating process based on plant specific data into the uncertainty analysis framework. In the following, we briefly summarize the possibility theory and address how to transform the belief and plausibility functions in a possibility distribution, and introduce the process of Bayesian updating of possibility distributions when new information is available.

Possibility theory [15] is relevant to represent consonant imprecise knowledge. The basic notion is the possibility distribution, denoted  $\pi$ , an upper semi-continuous mapping from the real line to the unit interval. A possibility distribution describes the more or less plausible values of some uncertain parameter  $X$ . Possibility theory provides two evaluations of the likelihood of an event, for instance whether the value of a real variable  $X$  lies within a certain interval: the possibility  $\Pi$  and the necessity  $N$  are defined as:

$$\Pi(A) = \sup_{x \in A} \pi(x) \quad (3-8)$$

$$N(A) = 1 - \Pi(\bar{A}) = \inf_{x \notin A} (1 - \pi(x)) \quad (3-9)$$

A unimodal numerical possibility distribution may also be viewed as a nested set of confidence intervals, which are the  $\alpha$ -cuts  $[x_\alpha, \bar{x}_\alpha] = \{x, \pi(x) \geq \alpha\}$  of  $\pi$ . The degree of certainty that  $[x_\alpha, \bar{x}_\alpha]$  contains  $X$  is  $N([x_\alpha, \bar{x}_\alpha]) = \alpha$  (if  $\pi$  is continuous). Conversely, a nested set of intervals  $A_i$  with degrees of certainty  $\lambda_i$  that  $A_i$  contains  $X$  is equivalent to the possibility distribution  $\pi(x) = \min\{1 - \lambda_i, x \in A_i, i = 1 \dots n\}$  provided that  $\lambda_i$  is interpreted as a lower bound on  $N(A_i)$ , and  $\pi$  is chosen as the least specific possibility distribution satisfying these inequalities [16].

We can interpret any pair of dual functions necessity/possibility  $[N, \Pi]$  as upper and lower probabilities induced from specific probability families.

Let  $\pi$  be a possibility distribution inducing a pair of functions  $[N, \Pi]$ . We define the probability family  $P(\pi) = \{p, \forall A \text{ measurable}, N(A) \leq p(A)\} = p, \forall A \text{ measurable}, p(A) \leq \Pi(A)\}$ . In this case,  $\sup_{p \in P(\pi)} p(A) = \Pi(A)$  and  $\inf_{p \in P(\pi)} p(A) = N(A)$  hold. In other words, the family  $p(\pi)$  is entirely determined by the probability intervals it generates.

Suppose pairs (interval  $A_i$ , necessity weight  $\lambda_i$ ) supplied by an expert are interpreted as stating that the probability  $p(A_i)$  is at least equal to  $\lambda_i$  where  $A_i$  is a measurable set. We define the probability family as follows:  $p(\pi) = \{p, \forall A_i, \lambda_i \leq p(A_i)\}$ . We thus know that  $\bar{p} = \prod$  and  $\underline{p} = N$ .

For a unimodal continuous possibility  $\pi$  with core  $\{a\}$  (i.e.  $\prod(\{a\}) = \pi(a) = 1$  and  $\forall x \neq a, \pi(x) \neq 1$ ), the set of probability measures  $P(\pi)$  can be more conveniently described by a condition on the cdfs of these probabilities, that is  $P(\pi) = \{p, \forall x, y, x \leq a \leq y, F(x) + 1 - F(y) \leq \max(\pi(x), \pi(y))\}$ . Note that we can choose  $x$  and  $y$  such that  $\pi(x) = \pi(y)$  in the expression of  $P(\pi)$ , i.e. suppose that  $[x, y]$  is a cut of  $\pi$ . If  $I_\alpha$  is the  $\alpha$ -cut of  $\pi$ , it holds that  $P(\pi) = \{p, p(I_\alpha) \geq N(I_\alpha), \forall \alpha \in (0, 1]\}$ .

Considering a particular probability box  $[F, \bar{F}]$  such

that  $\overline{F}(x) = \mathbb{I}(X \in (-\infty, x])$  and  $\underline{F}(x) = N(X \in (-\infty, x])$ , it is clear that

$$\overline{F}(x) = \begin{cases} \pi(x) & \text{for } x \leq a \\ 1 & \text{for } x \geq a \end{cases} \quad (3-11)$$

$$\underline{F}(x) = \begin{cases} 0 & \text{for } x \leq a \\ 1 - \pi(x) & \text{for } x \geq a \end{cases} \quad (3-10)$$

The probability box  $[\underline{F}, \overline{F}]$  above has an important specific feature; there exists a real value  $a$  such that  $\overline{F}(a) = 1$  and  $\underline{F}(a) = 0$ . It means that the p-box contains the deterministic value  $a$ , so that the two cdfs are acting in disjoint areas of the real line separated by this value. We can retrieve a possibility distribution from such two cdfs as  $\pi = \min(\overline{F}, 1 - \underline{F})$  and, thus, retrieve the possibility distribution that generated the p-box.

Once we use Equations (3-6) and (3-7) to build the belief and plausibility functions of parameter  $X$  based on industry generic data expressed in a form  $[m, \mu, M]$ , where  $\mu$  is the mean and  $m, M$  are, respectively, the lower bound and the upper bound, we can transform them to a prior possibility distribution such that  $\pi(x) = (M - \mu)/(M - x)$  for  $x \in [m, \mu]$  and  $\pi(x) = 1 - (x - \mu)/(x - M)$  for  $x \in [\mu, M]$ , as we discussed above. The prior possibility distribution is a unimodal continuous distribution with core  $\{\mu\}$ .

The objective of Bayesian updating is to calculate the posterior possibility distribution  $\pi(x|y)$  of  $X$  after  $y$  is obtained. To this aim, we employ a method based on a purely possibilistic counterpart of the classical, probabilistic Bayes' theorem [17]:

$$\pi(x_i|y) = \frac{\pi^L(x_i|y)\pi(x_i)}{\max[\pi^L(x_i|y)\pi(x_i)]} \quad \text{for } i = 1 \dots n \quad (3-12)$$

where  $\pi^L(x_i|y)$  is the possibilistic likelihood of the parameter  $X$  given the newly observed data  $y$ , and quantities  $\pi(x|y)$  and  $\pi(x)$  are defined above. Notice that  $\max[\pi^L(x_i|y)\pi(x_i)]$  is a normalization factor such that  $\max[\pi(x|y)] = 1$ , as required by possibility theory [18].

The posterior possibility distribution  $\pi(x|y)$  thereby obtained is also a unimodal continuous distribution. Then, we can obtain the corresponding belief and plausibility functions using Equations (3-10) and (3-11).

#### 4. DST OF EVIDENCE FOR UNCERTAINTY REPRESENTATION AND PROPAGATION IN NPP SPRA

The construction of belief functions within the DST does not rely on any assumption and is carried out directly from the original data. In this section, we describe the typical characteristics of the data available for SPRA and show how to build Dempster-Shafer structures based on this (limited) information.

#### 4.1 Building Dempster-Shafer structure of Seismic Hazard Curves

As mentioned earlier, most NPP SPRA models use only a single hazard curve (50% percentile or mean); this implies that we treat the ground motion parameter (i.e. PGA) as a random (aleatory) variable, only. However, the seismic hazard experts provide more than one hazard curve to represent the uncertainty bounds based on their knowledge; we can, then, build the corresponding Dempster-Shafer structures for the ground motion parameter (i.e. PGA) following these steps:

- Transform each hazard curve to a PGA cumulative density function, given an earthquake has occurred.
- Discretize the lower (i.e. 10%) and upper (i.e. 90%) PGA cumulative density functions to generate the focal intervals and corresponding masses (notice the focal intervals may overlap).
- Subdivide each focal interval by another percentile (e.g. 50%) PGA cumulative density function and distribute the mass of each focal interval to the two (new) focal intervals thereby originated; the subdivided focal intervals in each focal interval will not overlap as shown on Figure 3-3.
- Integrate all subdivided focal intervals to build the final Dempster-Shafer structure.

As mentioned in section 2.1, the  $x\%$  percentile curve defines the motion level that we are  $x\%$  confident that it will not be exceeded. If the bounding curves (i.e.  $x = 0$  and  $x = 100$ ) exist, we can define the uncertainty bound. Unfortunately, this is not always true in practice; in this case, we can take the lowest (e.g. 10%) and highest (e.g. 90%) as bounds, and this is the only assumption we make in the whole analysis framework. The process of converting the hazard curve to a cdf and, then, building the Dempster-Shafer structure will be shown in section 5.

#### 4.2 Building the Dempster-Shafer Structure of Seismic Fragility Curves

Traditionally, most NPP SPRA models use mean fragility curves to represent the conditional failure probability of a component. For a given PGA value, the conditional failure probability calculated by Equation (2-1) (replacing  $\beta_R$  with  $\beta_C$ ) is just a point value. This implies that the component fragility parameters do not contribute to the epistemic uncertainty. For a given PGA value, the conditional failure probability, calculated by Equation (2-2), is a single curve, which means that we have perfect knowledge about the probability and we can treat fragility as a random (aleatory) variable. However, for a given PGA focal interval  $[a_m, a_M]$ , we can directly build the Dempster-Shafer structure of the component failure probability based on  $A_m, \beta_R$ , and  $\beta_U$  by Equation (2-2).

Figure 4-1 is an example of the Dempster-Shafer structure of component conditional failure probability, given the PGA focal interval  $[0.2g, 0.3g]$ . The number of

component failure probability focal intervals is 20 and the mass of each is 5%. The lower bound is calculated by setting confidence level  $Q_L = [0.005, 0.05, 0.1, \dots, 0.95]$  and the upper bound is calculated by setting confidence level  $Q_U = [0.05, 0.1, \dots, 0.95, 0.995]$ .

### 4.3 Building the Dempster-Shafer Structure of Component Failure Probabilities

The generic data of component reliability provided by industry data banks usually contain mean values and presumed distribution parameters. Thus, the data of an input parameter  $X$  can be typically expressed in a form  $[m, \mu, M]$ , where  $\mu$  is the mean and  $m, M$  are, respectively, the lower bound and the upper bound. The value of  $m$  and  $M$  can be obtained directly from the 5% and 95% percentiles of the 90% confidence interval. Hence the Dempster-Shafer structure of the parameter based on generic data can be built by Equation (3-6) and (3-7), as shown in Figure 3-4.

In the traditional PRA practice, collected plant specific data is used to provide more information to reduce the uncertainty in the parameter estimate. In case we use the Dempster-Shafer structure to represent the epistemic uncertainty in the parameters, the plant specific data is used to reduce the epistemic uncertainty and narrow down the focal intervals using the method described in section 3.3.

### 4.4 Uncertainty Propagation through the Logic Model

This step consists of propagating the uncertainty in the input parameters (seismic hazard curves, seismic fragility curves, component failure probabilities,...) through the logic model of the system (i.e. the SET) in order to estimate the CDF of the NPP of interest. In the Dempster-Shafer framework, the propagation of uncertainties is not as straightforward as for the probabilistic approach as it consists of propagating focal intervals. When the input parameters are independent, the uncertainties are propagated by performing the Cartesian product of the input focal intervals and propagating them, the probability mass of the resulting output focal intervals is obtained using the product of the probability masses of the input intervals.

## 5. CASE STUDY

In this section, we refer to a simplified model to demonstrate the whole SPRA uncertainty assessment process. The scheme of the hypothetical (simplified) NPP sketched in Figure 5-1 is located in a seismic area characterized by the seismic hazard curves of Figure 5-2 [19]. The fragility curves parameters for the 14 components of the simplified NPP are given in Table 5-1 [20], and the components generic and specific data available is provided in Table 5-2 [2, 21].

The corresponding SET is shown in Figure 5-3: OSP is offsite power system; EDG represents emergency diesel generator system including day tank (EDGDT), diesel generator (EDGDG), fuel storage tank (EDGST), fuel

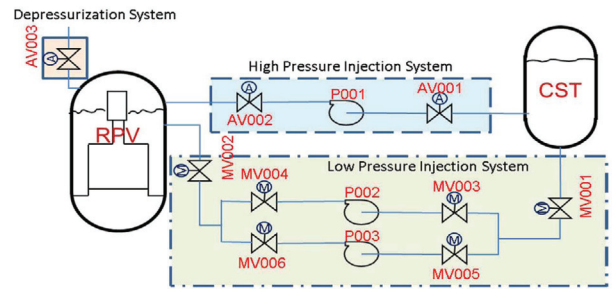


Fig. 5-1. Simplified NPP Layout

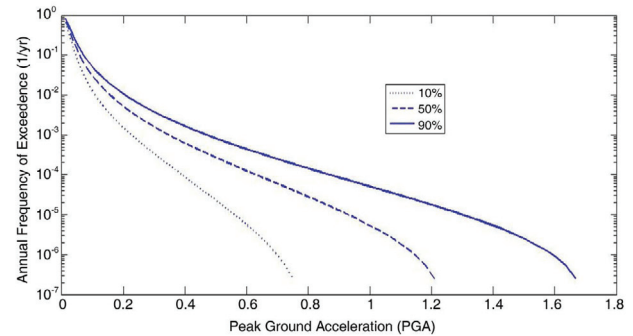


Fig. 5-2. Seismic Hazard Curves

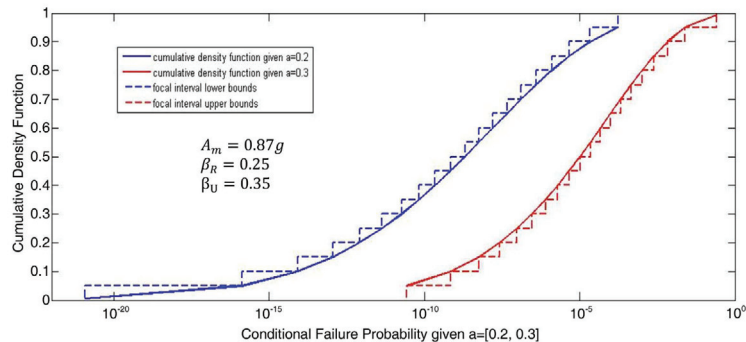


Fig. 4-1. Example of DST Structure for Component Failure Probability

**Table 5-1.** Parameters of Component Fragility Curves

|       | Structure/Component                   | $A_m$ | $\beta_R$ | $\beta_U$ |
|-------|---------------------------------------|-------|-----------|-----------|
| OSP   | Offsite Power Transformers            | 0.3   | 0.39      | 0.39      |
| EDGDT | Fuel Oil Day Tank                     | 2.33  | 0.36      | 0.38      |
| EDGDG | Emergency Diesel Generator            | 3.4   | 0.33      | 0.39      |
| EDGST | DG Fuel Oil Storage Tank              | 2.39  | 0.18      | 0.13      |
| EDGFP | EDG Fuel Transfer Pump                | 6.9   | 0.29      | 0.31      |
| EDGSA | EDG Starting Air Receivers            | 8.58  | 0.3       | 0.42      |
| CST   | Condensate Storage Tank               | 1.1   | 0.33      | 0.33      |
| HPCPI | High Pressure Injection System Piping | 4.02  | 0.38      | 0.43      |
| HPCPP | High Pressure Injection System Pumps  | 4.75  | 0.31      | 0.41      |
| SRV   | Safety Relief Valve                   | 3.8   | 0.43      | 0.43      |
| RHRPI | RHR System Piping                     | 4.02  | 0.38      | 0.43      |
| RHRPP | RHR Pumps                             | 3.48  | 0.31      | 0.41      |
| RHRHX | RHR Heat Exchangers                   | 8.8   | 0.38      | 0.46      |

**Table 5-2.** Component Reliability Data

| Basic Event | Industry Data |        |        | Specific Data |                             |
|-------------|---------------|--------|--------|---------------|-----------------------------|
|             | 5%            | mean,  | 95%    | # of failure  | # of demand (running hours) |
| AVD         | 6.0E-5        | 1.2E-3 | 4.0E-3 | 7             | 8844                        |
| MVD         | 8.0E-5        | 1.0E-3 | 3.0E-3 | 9             | 9052                        |
| PMA         | 6.0E-5        | 1.5E-3 | 5.0E-3 | 9             | 4538                        |
| PME         | 5.0E-5        | 4.0E-4 | 1.0E-3 | 2             | 3329.8h                     |
| HR-ADS      | 1.3E-4        | 3.4E-3 | 1.3E-2 | --            | --                          |

transfer pump (EDGFP) and starting air receiver (EDGSA); CST is the condensate storage tank; HP represents high pressure coolant injection system including system piping (HPCPI) and pump (HPCPP); SRV represents the safety relieve valve and LP represents low pressure coolant injection system including system piping (RHRPI), pump (RHRPP) and heat exchanger (RHRHX).

There are 8 sequences in the SET. Notice that since the median capacity  $A_m$  of the OSP is much smaller than the others (see Table 5-1), if the offsite power system survives after the earthquake, it is very likely that the other systems also survive. Thus, even if a transient occurs under this condition, there are still many safety systems that can mitigate the transient and can lead the reactor to a safe state. Thus, the final plant state for sequence 1 is set directly to ‘OK’ in case of OSP success (Sequence 1). Instead, if the OSP and EDG fail simultaneously (Sequence 8), we conservatively assume that the core will be damaged,

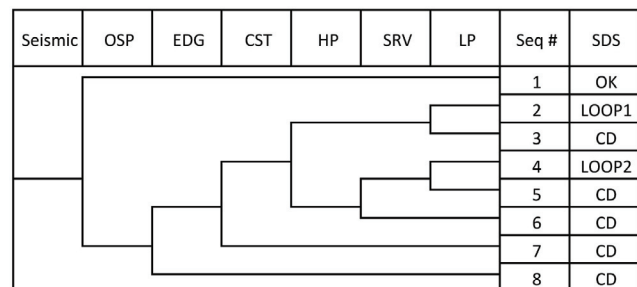


Fig. 5-3. Seismic Event Tree

although there are some additional safety systems that can intervene.

The other sequences reflect the scenarios possibly generated by the LOOP event. The SDS of Sequences 3, 5, 6 and 7 are ‘CD’ due to loss of coolant injection (Sequences 5, 6 and 7) or long term cooling (Sequence 3). Since Sequence 2 (LOOP1) and Sequence 4 (LOOP2) still have other systems available to mitigate the seismic events, they must be combined with the internal event trees to consider the contribution of non-seismic failures.

### 5.1 Seismic Hazard Curves

A tabular presentation of the hazard curves (Figure 5-1) is also provided by the seismic hazard experts [19]. There are 166 point values for each hazard curve, partially shown in Table 5-3 (first 12 and last 10 points). The high-confidence -of-low-probability-of-failure (HCLPF) capacity of the weakest component (i.e. OSP) is 0.083g. This means that we can assume the reactor still operates normally

**Table 5-3.** Tabular Data of Hazard Curves

| Annual probability of exceedance | PGA (g) |        |        |
|----------------------------------|---------|--------|--------|
|                                  | 10%     | 50%    | 90%    |
| 8.11E-01                         | 0.0082  | 0.0106 | 0.0129 |
| 5.57E-01                         | 0.0149  | 0.0187 | 0.0224 |
| 3.81E-01                         | 0.0213  | 0.0264 | 0.0314 |
| 2.71E-01                         | 0.0269  | 0.0334 | 0.0398 |
| 2.01E-01                         | 0.0321  | 0.0400 | 0.0479 |
| 1.54E-01                         | 0.0368  | 0.0463 | 0.0557 |
| 1.22E-01                         | 0.0412  | 0.0522 | 0.0633 |
| 9.85E-02                         | 0.0452  | 0.0580 | 0.0708 |
| 8.11E-02                         | 0.0492  | 0.0637 | 0.0782 |
| 6.80E-02                         | 0.0529  | 0.0691 | 0.0854 |
| 5.77E-02                         | 0.0564  | 0.0745 | 0.0926 |
| 4.94E-02                         | 0.0599  | 0.0799 | 0.0998 |
| ...                              | ...     | ...    | ...    |
| 3.18E-06                         | 0.6355  | 1.0532 | 1.4710 |
| 2.79E-06                         | 0.6433  | 1.0654 | 1.4875 |
| 2.41E-06                         | 0.6516  | 1.0781 | 1.5047 |
| 2.06E-06                         | 0.6605  | 1.0916 | 1.5228 |
| 1.72E-06                         | 0.6702  | 1.1060 | 1.5419 |
| 1.39E-06                         | 0.6810  | 1.1216 | 1.5623 |
| 1.09E-06                         | 0.6930  | 1.1387 | 1.5844 |
| 7.95E-07                         | 0.7072  | 1.1580 | 1.6087 |
| 5.17E-07                         | 0.7249  | 1.1804 | 1.6358 |
| 2.52E-07                         | 0.7500  | 1.2086 | 1.6673 |

when the ground motion is lower than this value. From this point of view, the annual probability of exceedance of the ground motion threshold is  $6.80E-2$  (see the tenth row of Table 5-3), since the PGA value of the 90% hazard curve is the first one larger than 0.083g. The lower bound of PGA value, then, is determined by the 10% hazard curve (i.e. 0.0529g) and the upper bound is set to the maximum PGA value (i.e. 1.6673g) that the plant site may be subjected to according to the seismic hazard experts.

As explained in section 4.1, in order to build the Dempster-Shafer structure for the hazard curves, first we transform each hazard curve into a PGA cdf conditional on the seismic event. This is achieved by calculating the frequencies between two neighborhood PGA point data and, then, normalizing them by the annual probability of

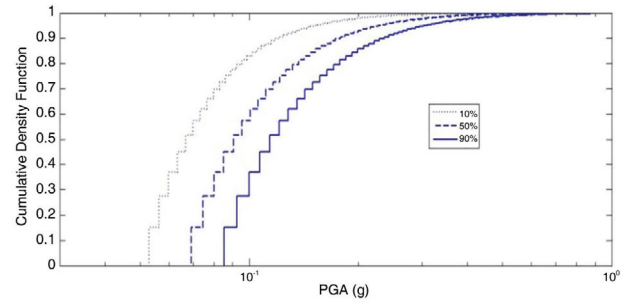


Fig. 5-4. PGA Cdfs Corresponding to the Seismic Hazard Curves of Figure 5-2

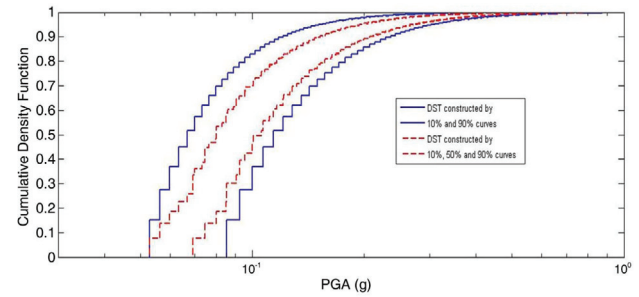


Fig. 5-5. Dempster-Shafer Structure of the Seismic Hazard Curves

exceedance of the ground motion (i.e.  $6.80E-2$ ) to obtain the probability densities of the PGA intervals. For example, according to the 10% hazard curve data in Table 5-3, the frequency between 0.0529g and 0.0564g is  $1.03E-2$  ( $= 6.80E-2 - 5.77E-2$ ) and the probability density of this PGA interval is  $1.51E-1$  ( $1.03E-2/6.80E-2$ ). After calculating the probability density for each interval, we can integrate them and obtain the corresponding cdfs as Figure 5-4.

Using the lower (i.e. 10%) and higher (i.e. 90%) PGA cdfs, we can generate the related Dempster-Shafer structure, i.e. the focal intervals and the corresponding masses (BBA) (solid lines in Figure 5-5). Then, using the additional information about the median, these focal intervals are further subdivided by the 50% curve and the Dempster-Shafer structure is reconstructed accordingly, as shown by the dashed lines in Figure 5-5.

### 5.2 Conditional Failure Probability of Top Events

There are six top events in the SET (see Figure 5-3). In this step, the fragility curves of each component are used to construct the Dempster-Shafer structure for each top event probability.

First of all, we represent the component fragility curves by Dempster-Shafer structures. As described in section 4.2, we can use fragility curves to calculate the bounds of each focal element and, then, build the Dempster-Shafer structure of the component failure probability given each PGA value of interest. An example of component fragility interval curves (OSP) is shown in Figure 5-6. In this Figure,

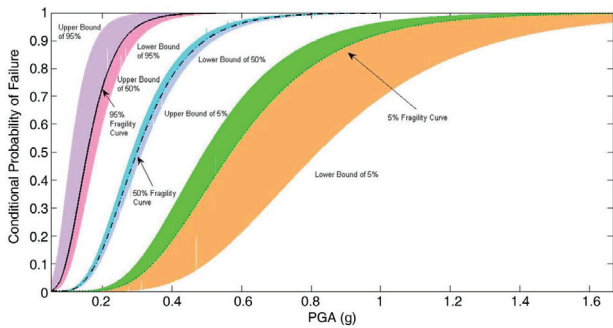


Fig. 5-6. Dempster-Shafer Structure of the Failure Probability of Component OSP for Different PGA Values

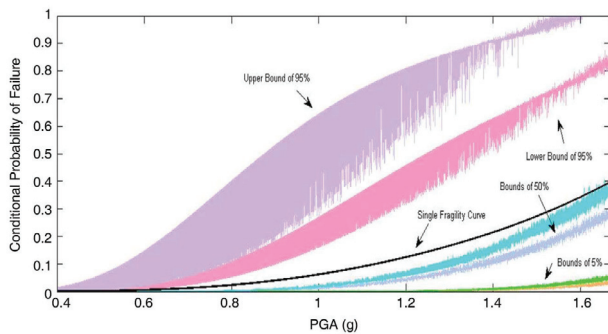


Fig. 5-7. Dempster-Shafer Structure for the Probability of Top Event EDG

the 5%, 50% and 95% percentile curves are shown, for a given PGA value. For comparison, the fragility curves calculated by Equation (2-2) are also plotted.

There are three top events consisting of only one component (i.e. OSP, CST and SRV): in this case, the top event level fragility interval curves are the same as the component fragility interval curves. For the other three top events (i.e. EDG, HP and LP), all the components fragility interval curves have to be propagated through the corresponding Fault Tree to get the top event level fragility interval curves. In this paper, the propagation has been carried out by standard Monte Carlo Simulation (MCS). The Dempster-Shafer structure corresponding to a given PGA value is, then, reconstructed according to the calculated focal intervals. An example of top event probability interval curves (for top event EDG) is shown in Figure 5-7; notice that the single fragility curve in the Figure (solid line) is the result of the traditional method combining the mean fragility curve (corresponding to parameters  $A_m$  and  $\beta_c$ ) of each component.

### 5.3 Conditional Probability of SDSs

This step propagates the fragility curves of the top events through the SET of Figure 5-3 to obtain the Dempster-Shafer structure of the probability of each SDS. There are four SDS (OK, LOOP1, LOOP2 and CD) in SET (see Figure 5-3). The equations of the sequence probabilities are shown in Table 5-4. The conditional probability of core

Table 5-4. SDS Equations

| Seismic Damage States | Equation                                    |
|-----------------------|---|
| OK                    | 1-OSP                                       |
| LOOP1                 | $OSP*(1-EDG)*(1-CST)*(1-HP)*(1-LP)$         |
| LOOP2                 | $OSP*(1-EDG)*(1-CST)*HP*(1-LP)$             |
| CD                    | $OSP*[1-(1-EDG)*(1-CST)*(1-LP)*(1-HP*SRV)]$ |

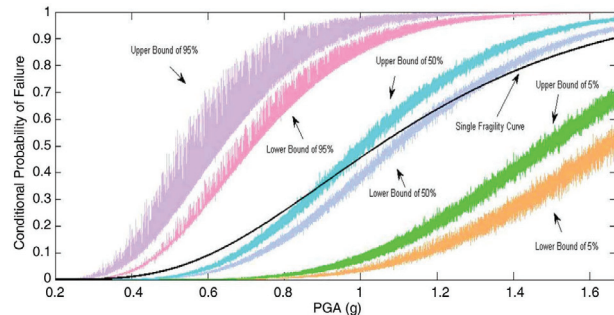


Fig. 5-8. Dempster-Shafer Structure for the Probability of SDS CD

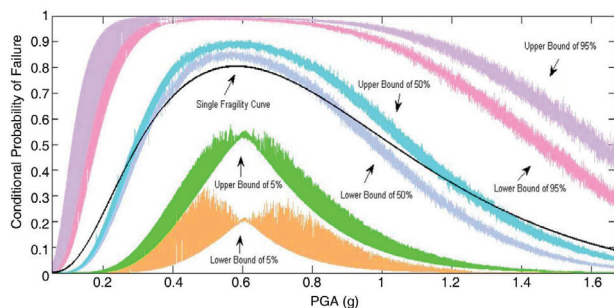


Fig. 5-9. Dempster-Shafer Structure for the Conditional Probability of Sequence LOOP1

damage directly induced by seismic (SDS CD) is shown in Figure 5-8 as a function of the different possible PGA values. Notice that the conditional failure probability monotonically increases with the ground motion as in the curve obtained by traditional methods.

The conditional probability curves of seismic initiating event LOOP1 are also shown in Figure 5-9. In this Figure, we can see that the conditional failure probability initially increases and, then, falls off with increasing PGA. This is due to the contribution of all the seismic initiating event sequences involving at least one safety system that operates successfully: the safety system success probabilities go to zero at high ground motions.

### 5.4 Conditional Probability of Core Damage Induced by Seismic Initiating Event Sequences

This step quantifies the conditional probabilities of core damage induced by seismic initiating event sequences.

| LOOP1 | HP | DP | LP | Seq # | End State |
|-------|----|----|----|-------|-----------|
|       |    |    |    | 1     | OK        |
|       |    |    |    | 2     | CD        |
|       |    |    |    | 3     | OK        |
|       |    |    |    | 4     | CD        |
|       |    |    |    | 5     | CD        |

Fig. 5-10. Internal Event Tree Corresponding to Seismic Initiating Event LOOP1

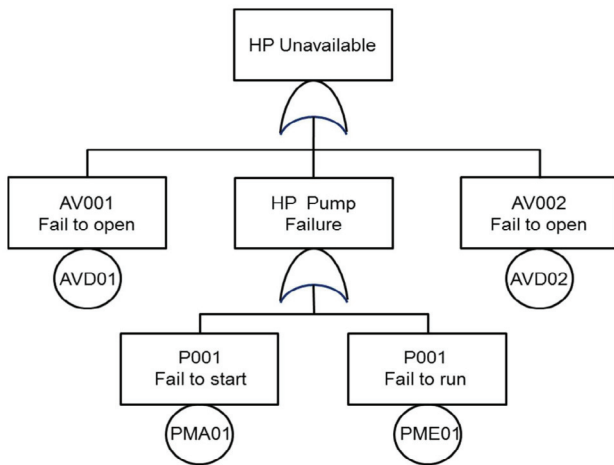


Fig. 5-11. The Fault Tree of Heading HP

In this step, the sequence probability curves for seismic initiating events (i.e. LOOP1 and LOOP2) have to be linked to the non-seismic event tree CCDP distribution bounds, so we need to build the Dempster-Shafer structure for the non-seismic event tree CCDP probability.

Taking seismic initiating event LOOP1 as an example, we build the corresponding internal event tree as in Figure 5-10. System fault trees are also constructed according to the simplified plant layout of Figure 5-1 to evaluate the probabilities of failure of system HP, DP and LP.

Before sequences quantification, we have to evaluate the failure probability for each safety system (headings HP, DP and LP) by means of the corresponding fault tree. For example, the HP fault tree (Figure 5-11) representing the logic of failure of the high pressure injection system, has to open two air-operated valves (AOV) and start the injection pump when receiving the auto-start signal: any of these components failing by demand and pump failing while running imply high pressure injection function failure. There are four basic events in the HP fault tree. The Dempster-Shafer structures for the failure probability of each basic component are constructed based on industry and plant data, (see Table 5-2) and then propagated through the fault tree to obtain the Dempster-Shafer structure for the failure probability of the safety system.

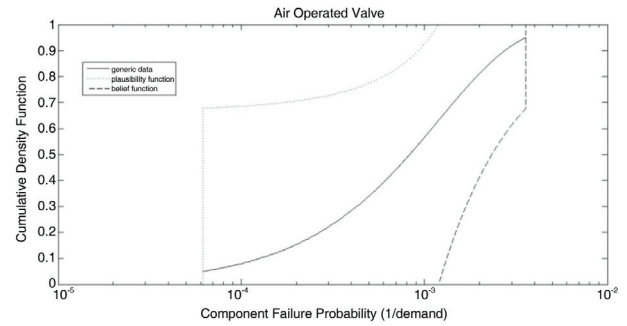


Fig. 5-12. The Belief and Plausibility Functions for the AOV Failure Probability

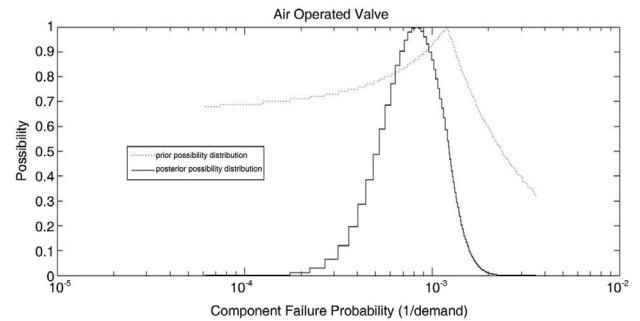


Fig. 5-13. Possibility Distributions for the AOV Failure Probability before (Dashed Line) and after (Solid Line) the Bayesian Update

According to the procedure already outlined in [14], first, we use the industry generic data to build the Dempster-Shafer structure for each basic event failure probability (Section 3.2). The 5-th and 95-th percentiles are set as the lower and upper bounds, respectively, of the uncertain probability ranges. The resulting belief and plausibility functions are shown in Figure 5-12 with reference to the AOV, only for illustration purposes. The predetermined (i.e. presumed) a priori beta function traditionally used in NPP PRAs to represent the AOV demand failure probability is also plotted in Figure 5-12, for comparison.

Then, the belief and plausibility functions constructed by means of the industry generic data are updated Bayesianly using the plant specific data available (Table 5-2). Thus, for Bayesian updating purposes, we transform the belief and plausibility functions into possibility distributions (Section 3.3). These possibility distributions are the prior possibility distributions used in the Bayesian update. As shown in Figure 5-13 with reference to the AOV failure probability, the left part of the prior possibility distribution coincides with the corresponding plausibility function, whereas the right part is equal to the complement of the corresponding belief function.

The prior possibility distributions are updated using the plant specific data by Equation (3-12). Continuing with the example, the posterior possibility distribution of the AOV failure probability is shown in Figure 5-13, for

comparison. It can be seen that after Bayesian update, the distribution is more peaked than before.

Finally, we reconvert the posterior possibility distribution of each basic event into belief and plausibility functions using Equations (3-10) and (3-11). Figure 5-14 shows the prior and posterior belief and plausibility functions for the AOV failure probability corresponding to the possibility distribution of Figure 5-13.

Once the Dempster-Shafer structures of the failure probability of all the basic events are built, they are propagated by the Monte Carlo simulation through the system internal event tree to obtain the Dempster-Shafer structure of the CCDP of seismic initiating events. The Monte Carlo uncertainty propagation for the LOOP1 CCDP is shown in Figure 5-15. In addition, for comparison purposes Figure 5-15 also reports the CCDP distributions obtained with the traditional Monte Carlo simulation using single (presumed and subjective) probability distributions for the basic events probabilities.

To construct the conditional probability intervals of core damage induced by the seismic initiating event of interest, we have to combine the Dempster-Shafer structure for each seismic initiating event (i.e. LOOP1 and LOOP2) with their associated CCDP bound. Again obtained by the MCS, the conditional probabilities of core damage induced by LOOP1 are shown as a function of PGA values in Figure 5-16.

### 5.5 Core Damage Probability

The probability curves of core damage induced by seismic initiating events are then combined with the sequence level fragility curves of core damage due directly to the seismic event in order to get the plant level core damage fragility curves (Figure 5-17): this means that for each ground motion value, the total conditional probability of core damage is obtained as  $CDP_{total} = CDP_{LOOP1} + CDP_{LOOP2} + CDP_{seismic}$ .

### 5.6 Core Damage Frequency

The final step is the estimation of the CDF. The total conditional probability curves for core damage are combined with the seismic hazard curves to complete the seismic risk assessment. The conditional probability bounds of core damage are obtained by sampling the PGA intervals constructed in Section 5.1. Figure 5-18 shows the final results and compares them with the traditional results obtained by employing the 50% hazard curve and mean component fragility curves.

We can see that a part of the traditional CDF result is not bounded by the bounding analysis. There are two reasons for this: first, the conditional probability of failure calculated by the mean component fragility curve is larger than 95% when ground motion value is small; second, using the 50% hazard curve neglects some contribution of low magnitude ground motion.

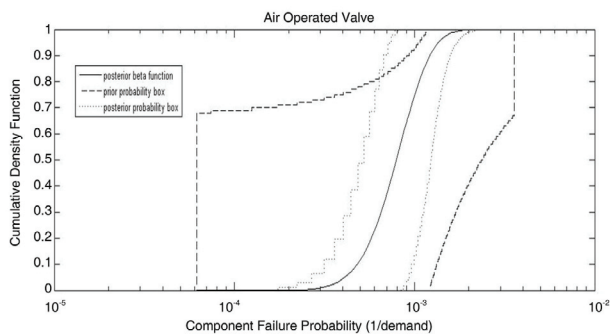


Fig. 5-14. The Prior and Posterior Probability Bounds for the AOV Failure Probability

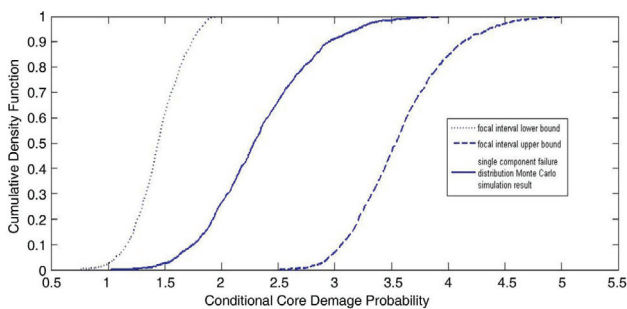


Fig. 5-15. The CCDP Bounds for Seismic Initiating Event LOOP1

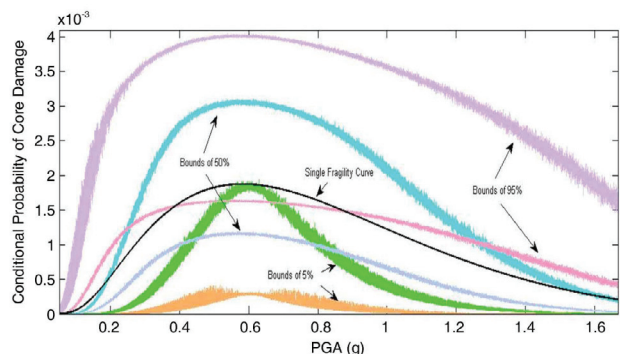


Fig. 5-16. The CCDP Induced by LOOP1 as a Function of Different PGA Values

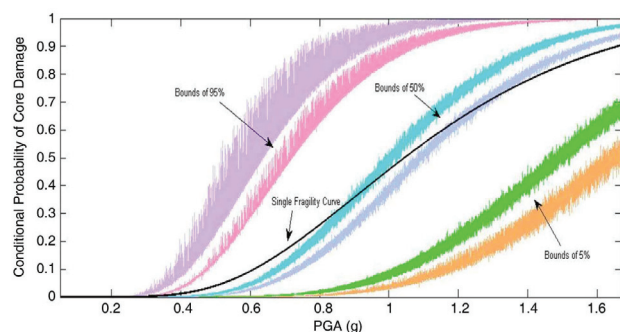


Fig. 5-17. Total Conditional Probability of Core Damage

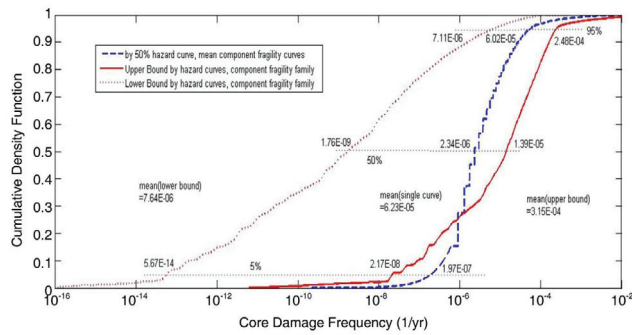


Fig. 5-18. CDF Results

## 6. SUMMARY AND CONCLUSION

The American Nuclear Society has developed a national standard [22] which provides requirements of three Capability Categories for conducting Probabilistic Risk Assessment of seismic events: Capability Category I can rely on generic or regional mean seismic hazard estimates and only a calculation of the mean CDF. Capability Category II requires a more thorough seismic hazard analysis and a full uncertainty analysis of the risk quantification. Capability Category III follows along the lines of the Seismic Safety Margin Research Program [23] and is likely considered only in a research program. In most practical cases, a calculation of the mean CDF (Capability Category I) is accepted to determine any changes in risk or in addressing Generic Safety Issues. For example, only a mean CDF estimate is required in IPEEE (Individual Plant Examinations of External Events) and, therefore, almost all of the IPEEE SPRA submittals would only comply with this requirement.

On the contrary, for confident decision making, more information is needed, in particular, addressing the (aleatory and epistemic) uncertainties affecting the SPRA.

The principal purpose of assessing uncertainty is to provide a reasonable assurance that the decisions are robust and would therefore not warrant reconsideration. In order to overcome the existing drawbacks of the traditional uncertainty analysis approaches in SPRA context, a DST framework for handling uncertainties has been proposed in this paper. This approach allows a representation and propagation of uncertainties that are coherent with the often limited information available on the system, and do not require arbitrary and subjective assumptions and distributions. In this paper, a demonstration of how to treat uncertainty using DST in SPRA has been given with reference to a simplified NPP. The procedure for building the Dempster-Shafer structures on the uncertain parameters based on generic data has been shown, the Bayesian updating based on specific data has also been introduced. The results have shown that the approach is feasible and effective in (i) describing and jointly propagating aleatory and epistemic uncertainties in SPRA models and (ii)

providing ‘conservative’ bounds on the safety quantities of interest (i.e. CDF) that reflect the (limited) state of knowledge of the experts about the system of interest. On the other hand, the presence of (possibly wide) uncertainty bounds makes the decision making process difficult, and this will be solved in future work.

## REFERENCES

- [1] EPRI, “Seismic Probabilistic Risk Assessment Implementation Guide,” EPRI-1002989, Electric Power Research Institute (2003).
- [2] S.A. Eide, T.E. Wierman, C.D. Gentillon, D.M. Rasmuson and C.L. Atwood, “Industry-Average Performance for Components and Initiating Events at U.S. Commercial Nuclear Power Plant,” NUREG/CR-6928, U.S. Nuclear Regulatory Commission Office of Nuclear Regulatory Research (2007).
- [3] C. Baudrit, I. Couso and D. Dubois, “Joint Propagation of Probability and Possibility in Risk Analysis: Towards a Formal Framework,” *International Journal of Approximate Reasoning*, vol. 45, pp. 82-105 (2007).
- [4] R.K. Durga, H. Hushwaha, A. Verma and A. Srividya, “Quantification of Epistemic and Aleatory Uncertainties in Level-1 Probabilistic Safety Assessment Studies,” *Reliability Engineering and System Safety*, vol. 92, pp. 947-956 (2007).
- [5] G. Shafer and G. Logan, “Implementing Dempster’s Rule for Hierarchical Evidence,” *Artificial Intelligence*, vol. 33, pp. 271-298 (1987).
- [6] S. Le Hegarat-Masclé, D. Richard and C. Otle, “Multi-Scale Fusion Using Dempster-Shafer Evidence Theory,” *Integrated Computer-Aided Engineering*, vol. 10, pp. 9-22 (2003).
- [7] T.D. Le Duy, L. Dieulle, D. Vasseur, C. Berenguer and M. Couplet, “An Alternative Framework Using Belief Functions for Parameter and Model Uncertainty Analysis in Nuclear Probabilistic Risk Assessment Applications,” *Proceedings of the Institution of Mechanical Engineers, Journal of Risk and Reliability* (2013).
- [8] SSHAC, “Recommendations for Probabilistic Seismic Hazard Analysis: Guidance on Uncertainty and Use of Experts,” NUREG/CR-6372, USNRC, Senior Seismic Hazard Analysis Committee (1997).
- [9] EPRI, “Methodology for Developing Seismic Fragilities,” EPRI-TR-103959, Electric Power Research Institute (1994).
- [10] G. Shafer, *A Mathematical Theory of Evidence*, Princeton University Press (1976).
- [11] A. Dempster, “Upper and Lower Probabilities Induced by a Multivalued Mapping,” *Annals of Mathematical Statistics*, vol. 38, pp. 325-339 (1967).
- [12] S. Ferson, L. Ginzburg, V. Kreinovich, D. Myers and K. Sentz, “Constructing Probability Boxes and Dempster-Shafer Structures,” SAND2002-4015, Sandia National Laboratories (2003).
- [13] S. Destercke, D. Dubois and E. Chojnacki, “Unifying Practical Uncertainty Representations: I. Generalized P-Boxes,” *International Journal of Approximate Reasoning*, vol. 49, pp. 649-663 (2008).
- [14] C.K. Lo, N. Pedroni and E. Zio, “Bayesian Probabilistic

- Analysis of a Nuclear Power Plant Small Loss of Coolant Event Tree Model with Possibilistic Parameters,” European Safety and Reliability Conference (ESREL 2013), Amsterdam, Netherland, Sep. 30 – Oct. 2, 2013.
- [15] D. Dubois and H. Prade, *Fundamentals of Fuzzy Sets*, Kluwer Academic Publication (2000)
- [16] D. Dubois and H. Prade, “When Upper Probabilities Are Possibility Measures,” *Fuzzy Sets and Systems*, vol. 49, pp. 65-74 (1992).
- [17] S. Lapointe and B. Bobeè, “Revision of Possibility Distributions: A Bayesian Inference Pattern,” *Fuzzy Sets and Systems*, vol. 116, pp. 119-140 (2000).
- [18] C. Baudrit and D. Dubois, “Practical Representations of Incomplete Probabilistic Knowledge,” *Computational Statistics & Data Analysis*, vol. 51(1), pp. 86-108 (2006).
- [19] C.H. Loh and K. L. Wen, “Seismic Hazard Re-Analysis of Taiwan Power Company’s Nuclear Power Plant No. 4 at Yenliao Site,” National Center for Research on Earthquake Engineering, 92B0600019 (2004)
- [20] C.C. Chao and M.C. Chen, “The Development of Seismic PRA Model for Lungmen Nuclear Power Plant,” Taiwan Power Company, NED-PRA-98A16815-REP-002-01 (2011)
- [21] INER, “PRA Model and Data Update for Kuosheng Nuclear Power Plant,” Institute of Nuclear Energy Research, (2004)
- [22] ANS, “American National Standard: External Events PRA Methodology,” ANSI/ANS 58.21 (2003).
- [23] USNRC, “Seismic Safety Margins Research Program, Phase I Final Report, SMACS – Seismic Methodology Analysis Chain with Statistics (Project VIII),” NUREG/CR-2015 (1981).